Microtubules in tau-expressing cells also have the same polarity[9]. Therefore, the polarity of microtubules in dendrites must be determined by factors other than interaction with MAP2 alone.

The mechanism underlying the bundling of microtubules by MAP2 and tau is likely to be complex[22,23]. Nonetheless, the present study clearly shows that in cells expressing a single brain MAP species, crossbridges between microtubules are formed whose length varies as a function of the length of the N-terminal arm. Furthermore, the inter-microtubule spacing also depends on the length of the N-terminal arm. Thus, the projection domains of these molecules seem likely to be key determinants of the spacing between microtubules in dendrites and axons. □

Received 6 August; accepted 23 October 1992.

1. Hirokawa, N. in *Neuronal Cytoskeleton* (eds. R. D. Burgoyne) 5–74 (Wiley Liss, New York, 1991).
2. Bernhardt, R. & Matus, A. *J. comp. Neurol.* **226,** 203–231 (1984).
3. Binder, L. I., Frankfurter, A. & Rebhun, L. I. *J. Cell Biol.* **101,** 1371–1378 (1985).
4. Matus, A. *A. Rev. Neurosci.* **11,** 29–44 (1988).
5. Nunez, J. *Trends Neurosci.* **11,** 477–479 (1988).
6. Kanai, Y. *et al. J. Cell Biol.* **109,** 1173–1184 (1989).
7. Lewis, S. A., Ivanov, I. E., Lee, G. H. & Cowan, N. J. *Nature* **342,** 498–505 (1989).
8. Knops, J. *et al. J. Cell Biol.* **114,** 725–733 (1991).
9. Baas, P. W., Pienkowski, T. P. & Kosik, K. S. *J. Cell Biol.* **115,** 1333–1344 (1991).
10. Umeyama, T., Okabe, S., Kanai, Y. & Hirokawa, N. *J. Cell Biol.* (in the press).
11. Takeuchi, M., Hisanaga, S., Umeyama, T. & Hirokawa, N. *J. Neurochem.* **58,** 1510–1516 (1992).
12. Goedert, M., Wischik, C. M., Crowther, R. A., Walker, J. E., & Klug, A. *Proc. natn. Acad. Sci. U.S.A.* **85,** 4051–5055 (1988).
13. Lee, G., Cowan, N. & Kirschner, M. W. *Science* **239,** 285–288 (1988).
14. Aizawa, H. *et al. J. biol. Chem.* **263,** 7703–7707 (1988).
15. Goedert, M., Spillantini, M. G., Potier, M. C., Ulrich, J. & Crowther, R. A. *EMBO J.* **8,** 393–399 (1989).
16. Kosik, K. S., Orecchio, L. D., Bakalis, S. & Neve, R. L. *Neuron* **2,** 1389–1397 (1989).
17. Lee, G., Neve, R. L. & Kosik, K. S. *Neuron* **2,** 1615–1624 (1989).
18. Papandrikopoulou, A., Doll, T., Tucker, R. P., Garner, C. C. & Matus, A. *Nature* **340,** 650–652 (1989).
19. Vallee, R. *Proc. natn. Acad. Sci. U.S.A.* **77,** 3206–3210 (1980).
20. Heidemann, S. R., Landers, J. M. & Hamborg, M. A. *J. Cell Biol.* **91,** 661–665 (1981).
21. Baas, P. W., Deitch, J. S., Black, M. M. & Banker, G. A. *Proc. natn. Acad. Sci. U.S.A.* **85,** 8335–8339 (1988).
22. Kanai, Y., Chen, J. & Hirokawa, N. *EMBO J.* **11,** 3953–3962 (1992).
23. Wille, H. *et al. J. struct. Biol.* **108,** 49–61 (1992).
24. Webb, N. R. & Summers, M. D. *MAXBAC™: Baculovirus Expression System. A Manual of Methods for Baculovirus Vectors and Insect Cell Culture Procedures* (Invitrogen, San Diego, 1990).
25. Sato-Yoshitake, R., Shiomura, Y., Miyasaka, H. & Hirokawa, N. *Neutron* **3,** 229–238 (1989).
26. Hirokawa, N. *J. Cell Biol.* **94,** 129–142 (1982).
27. Hirokawa, N., Shiomura, Y. & Okabe, S. *J. Cell Biol.* **107,** 1449–1461 (1988).
28. Hirokawa, N., Hisanaga, S. & Shiomura, Y. *J. Neurosci.* **8,** 285–306 (1988).

ACKNOWLEDGEMENTS. This work was supported by a grant-in aid for special project research by the Ministry of Education Science and Culture of Japan to N.H. and a HFSP grant to N.J.C. and N.H.

The spatial arrangement of cones in the primate fovea

J. D. Mollon* & J. K. Bowmaker†

* Department of Experimental Psychology, University of Cambridge, Cambridge CB2 3EB, UK
† Institute of Ophthalmology, University of London, Bath Street, London EC1V 9EL, UK

THE retinae of Old World primates contain three classes of light-sensitive cone, which exhibit peak absorption in different spectral regions[1–4]. But how are the different types of cone arranged in the hexagonal mosaic of the fovea? This question has often been answered with artists' impressions[5–7], but never with direct measurements. Staining for antibodies specific to the short-wave photopigment has revealed a sparse, semiregular array of cones[8]; but nothing is known about the arrangement of the more numerous long- and middle-wave cones. Are they randomly distributed, with chance aggregations of one type, as Hartridge postulated in these columns nearly 50 years ago[9,10]? Or do they exhibit a regular alternation, recalling the systematic mosaics seen in some non-mammalian species[6,11]? Or, conversely, is there positive clumping of particular cone types, as might be expected if local patches of cones were descended from a single precursor cell? We have made direct microspectrophotometric measurements of patches of foveal retina from Old World monkeys, and report here that the distribution of long- and middle-wave cones is locally random. These two cone types are present in almost equal numbers, and not in the ratio of 2:1 that has been postulated for the human fovea.

Post-mortem tissue was made available to us from talapoin monkeys (*Cercopithecus talapoin*) that had been used in unrelated endocrinological studies. When the fresh retina was dissected under dim red light, the fovea was usually visible as a dark spot. A retinal fragment that included the fovea was mounted on a slide, was divided by two or three strokes of a razor blade, and was then partially dispersed by gentle pressure on a cover slip. On occasion we were able to produce small fragments of intact retina that were suitable for microspectrophotometry and yet were extensive enough to answer the present question. The absorbance spectra of individual receptors were measured with a modified dual-beam Liebman microspectrophotometer under computer control[12–14]; the numerical apertures of the condenser and objective were 0.4 and 0.9, respectively[4]. With the help of an infrared converter, the measuring beam (2 μm square cross-section) was aligned so as to pass axially through a given cell while the reference beam passed either outside the retinal fragment or in a space between photoreceptors. The spectrum was scanned from 750 to 370 nm and back to 750 nm. To minimize the effects of bleaching, only one absorption spectrum was usually obtained from a given cell, but two independent estimates of the baseline absorbance spectrum were always obtained by arranging both beams to pass outside the cell. In the case of cells that absorbed at short wavelengths, we checked that the pigment was photolabile by repeating the absorbance measurements after bleaching the cell with white light for 5 min.

We were able to measure 30–40 receptors in a given patch. Although microspectrophotometric measurements are usually made by passing the beam transversely through the outer segment[15], our measurements of cells in these foveal patches were necessarily axial; the absorption spectra may thus be subject to minor distortion by inert pigments in the inner segments[4], by waveguide effects, or by scattering in other retinal tissue. Nevertheless, we were always able to assign a cone to one of three categories without ambiguity. In Fig. 1 we plot the wavelength of peak sensitivity (λ_{max}) for each of the long- and middle-wave cones recorded in the present study, including those used to construct Fig. 2: there is a clear separation of cones into two distinct classes and so we can be confident that our axial records are adequate for the present purpose of classification.

In Fig. 2 we show at the upper right a typical fragment of foveal retina from one of our preparations. The solid outline encloses the subset of the array that we were able to characterize

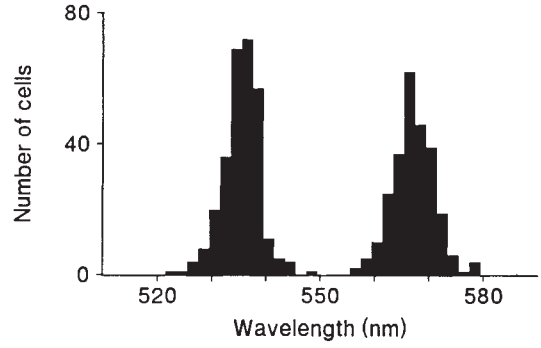

FIG. 1 The distribution of λ_{max} values for all middle- and long-wave cones in our sample, including those used in the construction of the schematic matrices of Fig. 2. For each individual record, the λ_{max} was estimated by fitting a template to the long-wave limb of the absorbance spectrum[4,14]. Note that we have included in this sample some records that would not pass our standard criteria[4] if our purpose were to establish the exact form of the mean absorbance spectrum. Nevertheless, the records fall into two distinct groups and there is no ambiguity in classifying individual cells as middle- or long-wave.

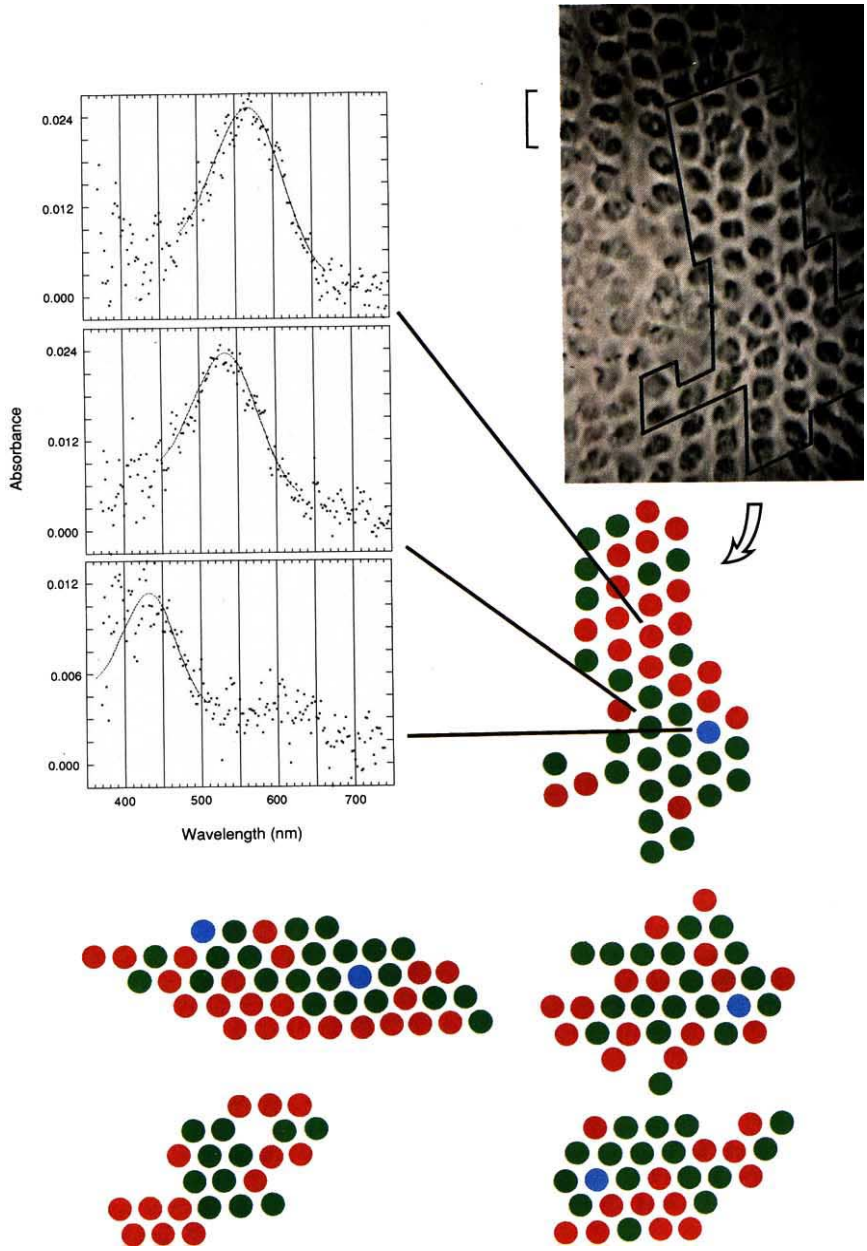

FIG. 2 The photograph at the upper right is of a fragment of fresh retina focused at the level of the outer segments and recorded on video by means of an infrared television camera permanently mounted on the microspectrophotometer. Scale bar, 10 μm. The solid outline encloses the area within which we measured each individual receptor. Immediately below the photograph, we show schematically the corresponding array of cones: long-, middle- and short-wave cones are represented by red, green and blue discs, respectively. For the three cones indicated, we show to the left their individual absorbance spectra, which are typical of those on which we base our classification; the solid curves fitted to the data are templates based on the Dartnall nomogram[13] displaced on a log frequency abscissa[4]. The lower part of the figure shows four other retinal patches that have been similarly analysed.

fully. To the left are shown examples of individual absorbance spectra for the three types of cones: the λ_{max} values lie close to 565, 535 and 430 nm, as is typical for Old World primates[1-4]. On the basis of similar spectra, we assigned each of a sample of 183 cones to one of three classes and so derived the matrices shown symbolically in the remainder of Fig. 2. The patches shown are drawn from five eyes from four female monkeys.

It is at once clear from Fig. 2 that the long- and middle-wave cones of the primate retina do not form the regular, systematically alternating array that has sometimes been postulated. Clumping of cones of the same type is apparent, but is this more than the chance aggregation that arises in any random distribution[9,16]? For the five patches shown, we have counted the transitions between two middle-wave cones, between two long-wave cones, and between cones of different types. The counts were made in one, arbitrary, direction (corresponding to the long axis of the fragment) and transitions involving short-wave cones were excluded. A χ^2 test showed that the frequencies of the three possible types of transition did not differ significantly from the values expected if the identity of a cone were independent of the identity of its neighbours and reflected only the absolute probability of that cone type ($\chi^2 = 1.22$, d.f. = 2). If there is any bias, it is towards aggregation rather than alternation.

Our finding that the foveal matrix is random rather than ordered has implications for the nature of the post-receptoral channels that subserve spatial and chromatic resolution. It would not be possible for the same midget ganglion cells to be optimized for both functions. Chromatic specificity of centre and surround inputs[17] would require that the ganglion cell's opposing inputs are not always drawn from cones that are nearest neighbours. Conversely, if spatial resolution is optimized in the sense that opposing inputs are drawn from neighbouring cones, then the surround inputs cannot always be drawn from a single class of cone[18]. In either case, the random clustering of cones of one type must constrain colour discrimination at high spatial frequencies, and also has implications for chromatic aliasing[7].

Of the 183 cones in our sample of intact retinal patches, long-wave, middle-wave and short-wave cones are present in the ratios 86:92:5 (47%, 50%, 3%). These records from intact patches are a subset of a total of 557 cones recorded from four male and six female talapoin monkeys. If we include all records (from intact patches and from isolated receptors) the corres-

ponding ratios are 256:289:12 (46%, 52%, 2%). The rarity of short-wave cones is concordant with earlier estimates, using direct and indirect means of identifying these receptors[1–4,8,19,20], but we have not ourselves seen any indication that the short-wave cones occur as interruptions to the regular foveal matrix, as has sometimes been reported[21]. The ratio of long- to middle-wave cones ranges from 1.6 to 0.42 for samples from individual animals and for the total sample has a value (0.89) that does not differ significantly from unity ($\chi^2 = 1.87$; d.f. = 1). This value is consistent with our earlier results for a number of catarrhine species[4] and with the results of Hárosi[3] and of Baylor, Nunn and Schnapf[2] for macaques, but it is extremely unlikely ($\chi^2 = 95$, d.f. = 1, $P < 0.001$) that our sample could be drawn from a population with a ratio of 2:1, the ratio that has been proposed for man on the basis of psychophysical measurements[22,23].

If this species difference proves to be real, two questions arise. First, what ecological factors have led to a more balanced proportion of long- and middle-wave cones in monkeys than in man? (Is it that good colour vision at small visual angles has been more important for frugivorous monkeys than for our own recent ancestors[24]?) Second, what is the molecular genetic mechanism that in monkeys leads to a near 1:1 ratio but in man to a strong bias in favour of long-wave cones? If we knew the answer to this question, we should be close to understanding the clinically important issue of how the expression of opsin genes is controlled. □

Received 10 August; accepted 5 October 1992.

1. Bowmaker, J. K., Dartnall, H. J. A. & Mollon, J. D. *J. Physiol.* **298,** 131–143 (1980).
2. Baylor, D. A., Nunn, B. J. & Schnapf, J. L. *J. Physiol.* **390,** 145–160 (1987).
3. Hárosi, F. I. *J. gen. Physiol.* **89,** 717–743 (1987).
4. Bowmaker, J. K. *et al. J. exp. Biol.* **156,** 1–19 (1991).
5. Walraven, P. L. *Vision Res.* **14,** 1339–1343 (1974).
6. Lythgoe, J. N. *The Ecology of Vision* (Oxford Univ. Press, Oxford, 1979).
7. Williams, D. R. *et al.* in *From Pigments to Perception* (eds Valberg, A. & Lee, B. B.) (Plenum, New York, 1991).
8. Curcio, A. C. *et al. J. comp. Neurol.* **312,** 610–624 (1991).
9. Hartridge, H. *Nature* **153,** 45–46 (1944).
10. Hartridge, H. *Nature* **157,** 482 (1946).
11. Bowmaker, J. K. & Kunz, Y. W. *Vision Res.* **27,** 2101–2108 (1987).
12. Liebman, P. A. & Entine, G. *J. opt. Soc. Am.* **54,** 1451–1459 (1964).
13. Knowles, A. & Dartnall, H. J. A. *The Photobiology of Vision* (Academic, London, 1977).
14. Mollon, J. D., Bowmaker, J. K. & Jacobs, G. H. *Proc. R. Soc.* B **222,** 373–399 (1984).
15. Dobelle, W. H., Marks, W. B. & MacNichol, E. F. Jr *Science* **168,** 1508–1510 (1969).
16. Hartridge, H. *Phil. Trans. R. Soc.* **232,** 519–671 (1947).
17. Reid, R. C., Shapley, R. M. *Nature* **356,** 716–718 (1992).
18. Lennie, P. & Haake, P. W., in *Computational Models of Visual Processing* (eds Landy, M. S. & Movshon, J. A.) 71–82 (MIT Press, Cambridge, MA, 1991).
19. Marc, R. E. & Sperling, H. G. *Science* **196,** 454–456 (1977).
20. de Monasterio, F. M., Schein, S. J. & McCrane, E. P. *Science* **213,** 1278–1281 (1981).
21. Anhelt, P. K., Kolb, H. & Pflug, R. *J. comp. Neurol.* **255,** 18–34 (1987).
22. Cicerone, C. M. & Nerger, J. L. *Vision Res.* **29,** 115–128 (1989).
23. Pokorny, J., Smith, V. C. & Wesner, M. F. in *From Pigments to Perception* (eds Valberg, A. & Lee, B. B.) (Plenum, New York, 1991).
24. Mollon, J. D. *J. exp. Biol* **146,** 21–38 (1989).

ACKNOWLEDGEMENTS. We thank M. Webster and B. C. Regan for discussion. Supported by the MRC and by Fight for Sight.

A cell line that can induce thymocyte positive selection

Patrice Hugo*, John W. Kappler*, Dale I. Godfrey† & Philippa C. Marrack*

* Howard Hughes Medical Institute, National Jewish Center for Immunology and Respiratory Medicine, 1400 Jackson Street, Denver, Colorado 80206, USA
† DNAX Research Institute of Molecular and Cellular Biology, Palo Alto, California 94304, USA

THE thymus positively selects thymocytes that bear T-cell receptors which recognize antigen presented by self major histocompatibility complex (MHC) proteins[1,2]. Positive selection is usually driven by MHC products on radiation-resistant cortical epithelial cells[3–5]. It is unknown whether positive selection is mediated by all thymic epithelial cells or by some specialized subsets[4]. Here we introduce an H-2^b-expressing thymic epithelial cell line into the thymuses of lethally irradiated H-2^k animals reconstituted with H-2$^{b/k}$ F_1 BM or fetal liver cells. I-A^b-restricted T cells are found in these animals, demonstrating that selection occurs on the introduced epithelial cells.

Long-term thymic cultures were established from C57BL/6 (H-2^b) mice. One clone, 2E4, was chosen on the basis of its reactivity with anti-cytokeratin antibodies. 2E4 cells were constitutively I-A^b-negative and bore low amounts of H-2K^b. High levels of both molecules were detected on 2E4 after interferon-γ (IFN-γ) treatment, an effect previously observed with other cultured thymic epithelial cells[6]. 2E4 cells did not express markers found on macrophages and dendritic cells, for example CD45, CD11a/18, HSA, CD11b/18, MAC-2, F4/80, and FcγRII/III. As for most cultured thymic epithelial lines, attempts to determine whether the 2E4 clone was derived from the cortex or the medulla were inconclusive.

2E4 cells pretreated with IFN-γ presented the superantigen staphylococcal enterotoxin B, which does not require processing, to the DO-11.10 T-cell hybridoma (Fig. 1). 2E4 cells presented chicken ovalbumin efficiently to BO-97.11, but very poorly to DO-11.10. But DO-11.10 was stimulated by the ovalbumin

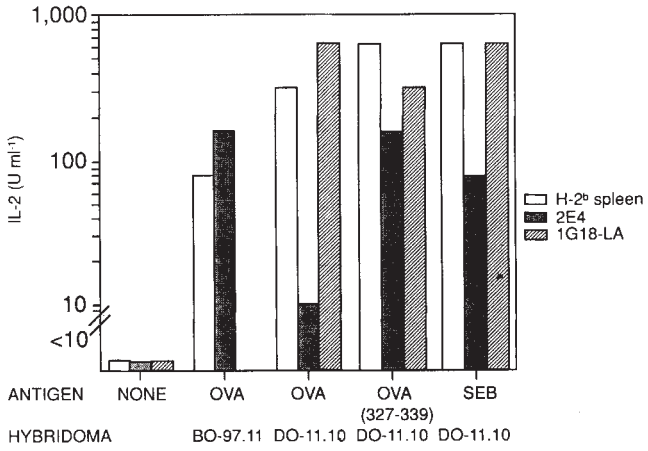

FIG. 1 Antigen presentation by 2E4 epithelial cells. The capacity of 2E4 cells (H-2^b) to present chicken ovalbumin (OVA), OVA peptide 327–339, and staphylococcal enterotoxin B (SEB) to T-cell hybridomas was compared to that of fresh splenocytes from C57BL/10 mice (H-2^b) or that of the thymic H-2^d macrophage cell line 1G.18LA.
METHODS. One of us (D.I.G.) established long-term cultures from thymuses of 6–8-week-old C57BL/6 female mice in α-MEM supplemented with 10% fetal calf serum, 10% horse serum, 5×10^{-5} M 2-mercaptoethanol and 5×10^{-7} M hydrocortisone. Cultures were passaged for several months and the 2E4 clone was obtained by two rounds of cloning and thereafter cultured in complete medium without hydrocortisone. Antigen presentation was assayed essentially as described[7]. Briefly, 2E4 and IG.18LA cells (gift from A. Zlotnik[7]) were plated in microculture plates (2.5×10^4 per well) and incubated in the presence of IFN-γ (200 U ml^{-1}) for 48 h. Cells were washed and OVA-specific T-cell hybridomas BO-97.11 (restricted by H-2^b) or DO-11.10 (restricted by H-2^b or H-2^d; TCR Vβ8.2$^+$) were added at 10^5 per well. Fresh splenocytes (10^6 per well) from C57BL/10 mice were also used as a source of antigen-presenting cells. Cultures were incubated for 24 h with 1 mg ml^{-1} OVA (Sigma), 30 μg ml^{-1} OVA peptide 327–339 (Macromolecular Resources) or 10 μg ml^{-1} SEB (Sigma). Interleukin 2 (IL-2) was assayed using HT-2 (ref. 21) and expressed as relative units per ml. No IL-2 was detected without preincubation of the 2E4 or 1G.18LA cells with IFN-γ.